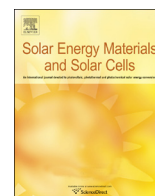




ELSEVIER

Contents lists available at [ScienceDirect](http://ScienceDirect)

## Solar Energy Materials &amp; Solar Cells

journal homepage: [www.elsevier.com/locate/solmat](http://www.elsevier.com/locate/solmat)Fabrication of ZnO/Cu<sub>2</sub>O heterojunctions in atmospheric conditions: Improved interface quality and solar cell performanceY. Ievskaya<sup>a,\*</sup>, R.L.Z. Hoye<sup>a</sup>, A. Sadhanala<sup>b</sup>, K.P. Musselman<sup>b</sup>, J.L. MacManus-Driscoll<sup>a</sup><sup>a</sup> Department of Materials Science and Metallurgy, University of Cambridge, 27 Charles Babbage Road, CB3 0FS, Cambridge, UK<sup>b</sup> Cavendish Laboratory, JJ Thomson Avenue, Cambridge CB3 0HE, UK

## ARTICLE INFO

## Article history:

Received 31 May 2014

Received in revised form

9 September 2014

Accepted 15 September 2014

Available online 3 October 2014

## Keywords:

Cuprous oxide

Spatial atmospheric ALD

ZnO/Cu<sub>2</sub>O heterojunction

Inorganic solar cell

## ABSTRACT

Zn<sub>1-x</sub>Mg<sub>x</sub>O/Cu<sub>2</sub>O heterojunctions were successfully fabricated in open-air at low temperatures via atmospheric atomic layer deposition of Zn<sub>1-x</sub>Mg<sub>x</sub>O on thermally oxidized cuprous oxide. Solar cells employing these heterojunctions demonstrated a power conversion efficiency exceeding 2.2% and an open-circuit voltage of 0.65 V. Surface oxidation of Cu<sub>2</sub>O to CuO prior to and during Zn<sub>1-x</sub>Mg<sub>x</sub>O deposition was identified as the limiting factor to obtaining a high quality heterojunction interface. Optimization of deposition conditions to minimize Cu<sub>2</sub>O surface oxidation led to improved device performance, tripling the open-circuit voltage and doubling the short-circuit current density. These values are the highest reported for a ZnO/Cu<sub>2</sub>O interface formed in air, and highlight atmospheric ALD as a promising technique for inexpensive and scalable fabrication of ZnO/Cu<sub>2</sub>O heterojunctions.

© 2014 The Authors. Published by Elsevier B.V. This is an open access article under the CC BY license (<http://creativecommons.org/licenses/by/3.0/>).

## 1. Introduction

Cuprous oxide (Cu<sub>2</sub>O) has recently received increasing attention as a low-cost abundant photovoltaic material (Fig. 1). Cu<sub>2</sub>O is a p-type semiconductor with a band gap of 2 eV and 23% theoretical efficiency limit [1]. However, the intrinsic nature of p-type conductivity in Cu<sub>2</sub>O makes the formation of a homojunction, and hence achieving maximum efficiency, difficult [2]. Most of the research effort has therefore been focused on heterojunction solar cells, pairing Cu<sub>2</sub>O with ZnO and its doped variations (see Table 1), although other wide band gap oxides such as In<sub>2</sub>O<sub>3</sub>:Sn (ITO), Ga<sub>2</sub>O<sub>3</sub> and TiO<sub>2</sub> have been investigated as well [3,4]. Fig. 1 and Table 1 present developments in Cu<sub>2</sub>O-based solar cell research over the past few years. One can note that the efficiencies and the open-circuit voltages of the devices have varied widely depending on the synthesis method used. In the most efficient cells, the p–n junction was formed by a vacuum-based technique such as pulsed laser deposition (PLD), atomic layer deposition (ALD) or sputtering. For low-cost photovoltaics, however, heterojunction synthesis outside a vacuum is preferable. Producing a good quality ZnO/Cu<sub>2</sub>O interface in open-air at low temperature and in a scalable manner remains a challenge. This work therefore utilizes a vacuum-free scalable technique, atmospheric atomic layer deposition (AALD), for the deposition of polycrystalline ZnO and Mg:ZnO thin films on cuprous oxide, itself made at atmospheric pressure.

Atmospheric (or spatial) ALD separates precursors in space rather than in time (cf. conventional ALD) and hence allows for quicker deposition of conformal oxide films for low-cost solar cells in a manner compatible with roll-to-roll processing [5]. In this work, optimal AALD conditions for the deposition of Zn<sub>1-x</sub>Mg<sub>x</sub>O were identified, in order to preserve the pristine surface of the Cu<sub>2</sub>O substrates and minimize the formation of phases detrimental to the heterojunction interface quality. When tested in solar cells, these optimizations resulted in a tripling of the open-circuit voltage (*V*<sub>oc</sub>) and doubling of the short-circuit current density (*J*<sub>sc</sub>), as well as an improved fill factor (FF), resulting in a six-fold increase in the power conversion efficiency (PCE) of the cells.

## 2. Experimental

## 2.1. Solar cell fabrication

Copper oxide substrates 13 mm × 13 mm × 170 μm were obtained by a 2 h oxidation of copper foil (0.127 μm thick, 99.9% pure, Alfa Aesar) at 1000 °C in an Ar–O<sub>2</sub> gas mixture, finished by quenching of the substrates from 500 °C in deionized water. The oxygen partial pressure was monitored throughout the heat treatment with a Rapidox 2100 Oxygen Gas Analyzer and was adjusted to approximately 10,000 ppm to keep the substrates in the phase region where cuprous oxide is thermodynamically stable. Cupric oxide formed on the substrate surface during quenching was removed by etching in dilute nitric acid [6], followed by sonication in isopropanol. Substrates

\* Corresponding author. Tel.: +44 1223 367919.

E-mail address: [yi241@cam.ac.uk](mailto:yi241@cam.ac.uk) (Y. Ievskaya).

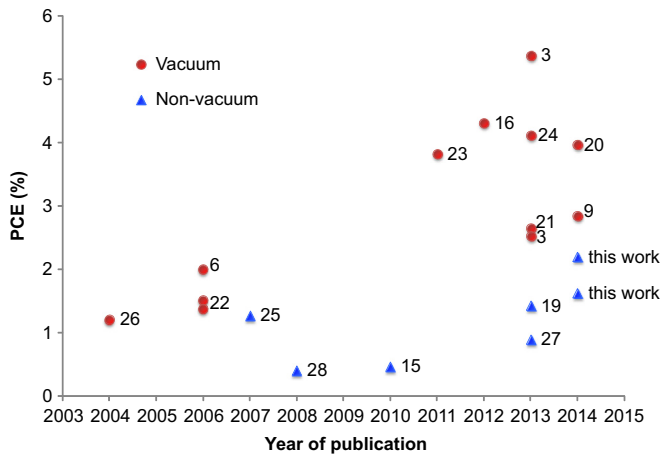


**Fig. 1.** Cu<sub>2</sub>O-based solar cell efficiency by year of publication. Markers indicate whether the interface was formed in vacuum or in atmosphere (non-vacuum). Efficiencies have remained low for atmospherically processed junctions, however, in this work, a PCE of 2% has been exceeded.

**Table 1**  
Cu<sub>2</sub>O-based solar cell efficiency latest developments (to 2014).

Type of junction	PCE %	V <sub>oc</sub> V	p–n junction formation	Ref.
<i>Cu<sub>2</sub>O-based junctions formed in vacuum</i>				
AZO/Ga <sub>2</sub> O <sub>3</sub> /Cu <sub>2</sub> O	5.38	0.8	PLD	[3]
AZO/Zn <sub>0.91</sub> Mg <sub>0.09</sub> O/Cu <sub>2</sub> O	4.3	0.8	PLD	[16]
AZO/ZnO/Cu <sub>2</sub> O	4.12	0.72	PLD	[24]
AZO/Ga <sub>2</sub> O <sub>3</sub> /Cu <sub>2</sub> O	3.97	1.2	ALD	[20]
AZO/ZnO/Cu <sub>2</sub> O	3.83	0.69	PLD	[23]
AZO/a-ZTO/Cu <sub>2</sub> O	2.85	0.62	ALD	[9]
AZO/a-ZTO/Cu <sub>2</sub> O	2.65	0.55	ALD	[21]
AZO/Cu <sub>2</sub> O	2.53	0.55	PLD	[3]
ITO/ZnO/Cu <sub>2</sub> O	2.01	0.6	IBS	[6]
ZnO:Ga/Cu <sub>2</sub> O	1.52	0.41	VAPE	[22]
AZO/Cu <sub>2</sub> O	1.39	0.4	dc-MSP	[22]
AZO/Cu <sub>2</sub> O	1.21	0.41	PLD	[26]
<i>Cu<sub>2</sub>O-based junctions formed without vacuum</i>				
ZnO/Cu <sub>2</sub> O	1.43	0.54	ECD	[19]
ZnO/Cu <sub>2</sub> O	1.28	0.59	ECD	[25]
ZnO/Cu <sub>2</sub> O/Cu <sub>2</sub> O <sup>+</sup>	0.9	0.32	ECD	[27]
ZnO/Cu <sub>2</sub> O	0.47	0.28	ECD	[15]
ZnO/Cu <sub>2</sub> O	0.41	0.32	ECD	[28]
<i>This study</i>				
ZnO/Cu <sub>2</sub> O	1.46	0.49	AALD	
ITO/Zn <sub>0.79</sub> Mg <sub>0.21</sub> O/Cu <sub>2</sub> O	2.2	0.65	AALD	

PLD – pulsed laser deposition, ALD – atomic layer deposition, ECD – electrochemical deposition, IBS – ion beam sputtering, VAPE – vacuum arc plasma evaporation, dc-MSP – direct current magnetron sputtering, a-ZTO – tin-doped zinc oxide, AZO – aluminum doped zinc oxide.

were then masked on one side with insulating black paint, defining the solar cell area to be approximately 0.1 cm<sup>2</sup>.

The zinc oxide and zinc magnesium oxide films were deposited using an Atmospheric ALD technique, similar to that described in [7]. Diethylzinc (DEZ) was used as the Zn precursor and bis(ethylcyclopentadienyl)magnesium as the Mg precursor. For zinc oxide deposition, the bubbling rate of nitrogen gas through the diethylzinc was 25 mL/min and the vapor was diluted with nitrogen carrier gas flowing at 100 mL/min. For zinc magnesium oxide deposition, the bubbling rate through the diethylzinc was 6 mL/min and 200 mL/min through the bis(ethylcyclopentadienyl)magnesium. The carrier gas flow rate was again 100 mL/min. Nitrogen gas was bubbled at 100 mL/min through deionized water, which was employed as the oxidant. This vapor was diluted with carrier gas flowing at 200 mL/min. Nitrogen was also flowed at

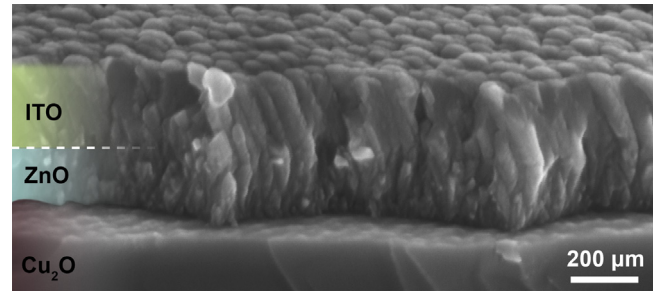


**Fig. 2.** Cross-sectional SEM image of ITO/ZnO/Cu<sub>2</sub>O heterojunction.

500 mL/min through the four channels spatially separating the oxidant and metal precursor channels in the AALD gas manifold. The ZnO deposition rate was approximately 0.4 nm per second (or per cycle).

A 180 nm thick top electrode was sputtered on top of the Zn<sub>1-x</sub>Mg<sub>x</sub>O film from an ITO (10% SnO<sub>2</sub>) target at the following conditions: power 20 W, base pressure < 10<sup>-9</sup> mbar, Ar pressure 2.5 Pa, sputtering rate 35 nm/min, sputtering time 5 min. Fig. 2 shows a cross-sectional SEM image of the ITO and ZnO films deposited on a thermally oxidized Cu<sub>2</sub>O substrate. An 80 nm gold bottom electrode was evaporated in an Edwards resistance evaporator (base pressure 8 × 10<sup>-6</sup> mbar, rate 0.8 Å/s). For the optimized Zn<sub>1-x</sub>Mg<sub>x</sub>O/Cu<sub>2</sub>O cells, the bottom electrode was evaporated before the formation of the p–n junction, as it was found that heating of the junction during evaporation leads to deteriorated performance. Top and bottom electrodes were contacted with Ag conductive paste for device testing.

## 2.2. Characterization

Surface and cross-sectional morphologies, as well as the composition of Cu<sub>2</sub>O substrates and solar cells were analyzed using a LEO VP-1530 field emission scanning electron microscope with a built-in Oxford Instruments detector for energy-dispersive X-ray spectroscopy (EDX).

Copper oxide absorption was measured by photothermal deflection spectroscopy (PDS). PDS is a highly sensitive surface averaged absorption measurement technique capable of measuring absorption 5–6 orders of magnitude weaker than the band-edge absorption. Detailed description of the PDS technique can be found elsewhere [8]. In this work, freestanding Cu<sub>2</sub>O samples were used for the PDS measurements.

Solar cells were tested under a simulated AM1.5G solar spectrum with the light intensity calibrated to 100 mW/cm<sup>2</sup> using a calibrated Si reference diode. The external quantum efficiency (EQE) of the cells was measured using a monochromator with a 100 W tungsten halogen lamp. The short-circuit current density obtained under the solar simulator was typically larger than the integrated short-circuit current density expected from the EQE measurements, which was attributed to different device performance with and without light soaking, underestimation of the device area, and spectral mismatch. To correct for this, all  $J_{sc}$  were scaled by a factor of 0.74 so that the integrated  $J_{sc}$  from the EQE and measured  $J_{sc}$  were in agreement.

## 3. Results and discussion

### 3.1. Cu<sub>2</sub>O surface instability

Thermally oxidized cuprous oxide is intrinsically unstable in air, always forming a thin CuO film on its surface [9,10]. It is evident from the Cu–O phase stability diagram that cupric oxide is

the stable phase at ambient conditions [11]. To probe the presence of CuO on Cu<sub>2</sub>O, as-oxidized and etched Cu<sub>2</sub>O substrates were examined with photothermal deflection spectroscopy (Fig. 3). The PDS absorption spectra for both substrates showed strong absorption at photon energies greater than ~2 eV, which is in agreement with the optical band gap of cuprous oxide. An absorption shoulder below the band gap (centered at ~1.6 eV) was present in both substrates. This shoulder can be attributed to the presence of cupric oxide (CuO), which has an optical band gap of approximately 1.4 eV [12]. The unetched Cu<sub>2</sub>O substrate had 10 times higher absorption in the 1.4–2 eV energy range than the etched substrate, implying a thicker CuO film on its surface, which was also confirmed visually as a grey semi-transparent film on the substrate. The fact that the freshly etched substrate also showed some absorption in this range suggests that a thin CuO film was still present on its surface when kept in ambient conditions, despite not being visually detectable.

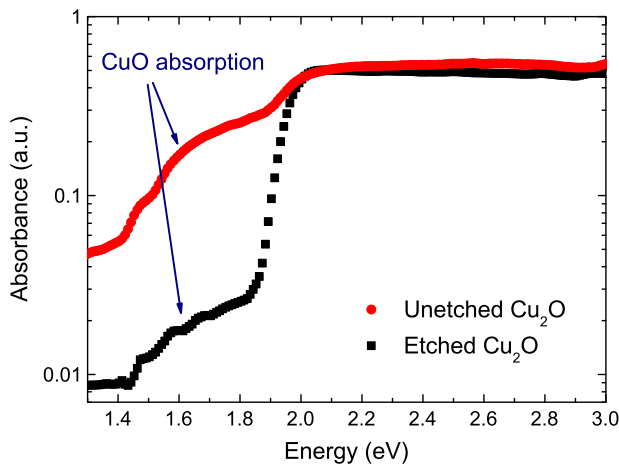


Fig. 3. PDS spectra of etched and unetched (as-oxidized) Cu<sub>2</sub>O substrates.

The etched cuprous oxide surface was found to be compromised even further when heated in air, which is necessary for the deposition of ZnO by AALD. Fig. 4 shows SEM images of an etched Cu<sub>2</sub>O substrate surface before (a) and after (b) annealing in atmosphere at 150 °C for 3 min on the AALD platen under nitrogen flow, but without a metal precursor or oxidant supplied to the substrate. The annealing temperature and duration were selected to replicate standard conditions used for the deposition of ZnO by AALD. As can be seen in Fig. 4a, the etched Cu<sub>2</sub>O surface was visibly ‘clean’, i.e. free from ~micron-sized second phases, featuring only the slip planes intersecting the surfaces of the differently oriented Cu<sub>2</sub>O grains. EDX analysis confirmed the chemical composition of the surface to be very close to that of Cu<sub>2</sub>O. However, after annealing (Fig. 4b), many micron-sized particles were found on the substrate surface. EDX analysis showed that the composition of these particles was close to that of CuO, while the composition of the adjacent substrate remained that of Cu<sub>2</sub>O. This suggests that cupric oxide growth is favored during the atmospheric deposition of metal oxides on a Cu<sub>2</sub>O surface.

Cupric oxide is an insulator and has a lower band gap (1.4 eV) than cuprous oxide (2 eV), which makes its presence undesirable for Cu<sub>2</sub>O photovoltaic applications: firstly, CuO absorbs radiation in the visible spectrum, thereby reducing the amount of photons reaching the Cu<sub>2</sub>O without contributing to the photocurrent. Secondly, the CuO conduction band, which is positioned approximately 4 eV below the vacuum level, introduces deep level trap states in the middle of the Cu<sub>2</sub>O band gap [9]. Cu<sup>2+</sup> defect states coming from CuO may promote recombination detrimental to the device performance.

On the positive side, CuO can be removed in an oxygen-free environment (e.g. via ion etching) immediately before the deposition of the n-type oxide or a buffer layer. Also, very thin (~nm) CuO film can be passivated or reduced to Cu<sub>2</sub>O with a reactive metal oxide precursor such as diethylzinc when deposited by conventional ALD [9]. However, when producing the heterojunction outside a vacuum, it is more difficult to eliminate CuO from

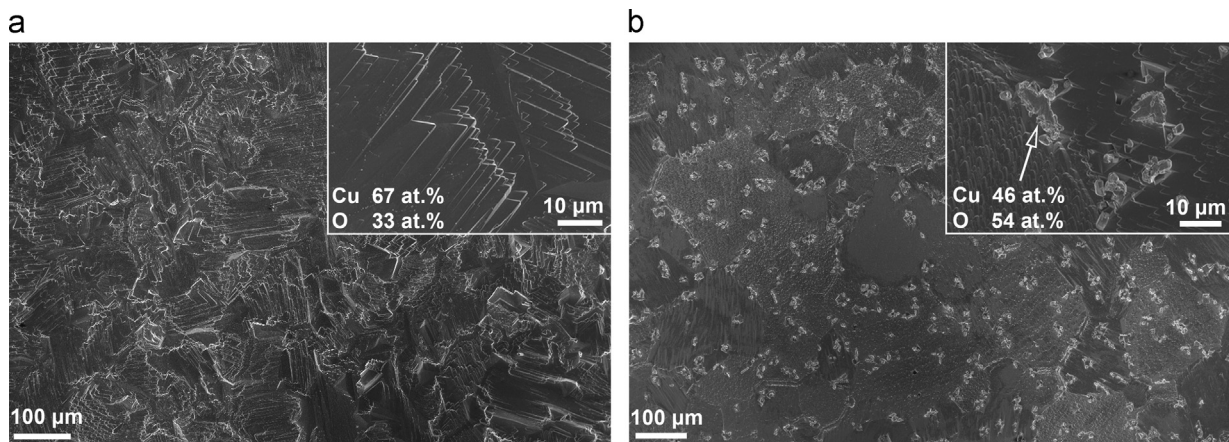


Fig. 4. SEM images of etched Cu<sub>2</sub>O surface before (a), and (b) after annealing at 150 °C in air on the AALD platen. Multiple CuO formations can be seen on the surface in (b). Insets with EDX measurements show the composition of the selected areas.

Table 2

Standard and optimized ZnO AALD deposition parameters and performance of the best corresponding ITO/ZnO/Cu<sub>2</sub>O solar cells.

ZnO/Cu <sub>2</sub> O solar cell	ZnO Deposition temperature (°C)	ZnO Deposition time (s)	$J_{sc}$ (mA/cm <sup>2</sup> )	$V_{oc}$ (mV)	FF (%)	PCE (%)
Standard	150	400	3.7	0.18	35	0.23
Optimized	100	100	7.5	0.49	40	1.46



the  $\text{Cu}_2\text{O}$  surface. While thick  $\text{CuO}$  can be removed by grinding and polishing [13] or chemical wet etching [14], as soon as the underlying cuprous oxide is re-exposed to air, cupric oxide forms on the surface again [9]. Indeed, we confirmed this by the PDS spectrum of the freshly etched  $\text{Cu}_2\text{O}$  substrate (Fig. 3). Therefore, in recognition of the chemical instability of  $\text{Cu}_2\text{O}$ , adaptation of the atmospheric deposition conditions used to deposit the n-type semiconductor is necessary.

### 3.2. AALD ZnO deposition optimization

$\text{ZnO}/\text{Cu}_2\text{O}$  solar cells made with  $\text{ZnO}$  films deposited under standard  $\text{ZnO}$  AALD conditions (see Table 2 and Fig. 6, “standard”) exhibited poor performance as compared to the values reported in literature for cells made by other methods (Table 1). The low open-circuit voltage in these devices was attributed to the presence of  $\text{CuO}$  and other copper compounds between the  $\text{Cu}_2\text{O}$  and  $\text{ZnO}$  layers. These undesirable phases can be seen as whisker- and flower-like formations in the SEM image of the surface of a standard  $\text{ZnO}/\text{Cu}_2\text{O}$  solar cell (Fig. 5a). The image indicates that the  $\text{CuO}$  particles formed on the substrate surface during the AALD deposition remain underneath the  $\text{ZnO}$  film and hinder the formation of a proper  $\text{ZnO}/\text{Cu}_2\text{O}$  heterojunction, significantly decreasing the attainable open-circuit voltage. Measures were therefore taken in order to minimize oxidation of the  $\text{Cu}_2\text{O}$  substrate during the deposition of the  $\text{ZnO}$ . The time the substrates spent on the hot platen in air directly before, during and after the deposition was minimized. The deposition temperature was also reduced to decrease the diffusion rate of oxygen through the  $\text{ZnO}$  to the heterojunction and therefore the  $\text{Cu}_2\text{O}$  oxidation rate. Additionally, in an attempt to reduce the surface  $\text{CuO}$  to  $\text{Cu}_2\text{O}$ , the oxidant was introduced to the substrate only after a few cycles of metal precursor, as reported previously in [9].

To determine the optimum deposition temperature and time,  $\text{ZnO}$  was deposited for 40 s, 100 s, 200 s and 400 s at 150 °C and at 50, 75, 100 and 150 °C for 100 s. Fig. 7 shows the correlation of the open-circuit voltage with the duration of the deposition (a) and deposition temperature (b). It can be seen that  $V_{oc}$ s tend to decrease towards higher deposition temperature and longer time. This is in agreement with  $\text{Cu}_2\text{O}$  surface instability discussed earlier, since prolonged annealing in air at elevated temperature results in further oxidation of  $\text{Cu}_2\text{O}$  to  $\text{CuO}$ . Similar findings were reported in literature, for example, Minami et al. have emphasized that to stabilize the  $\text{Cu}_2\text{O}$  surface, a TCO has to be deposited as quickly as possible, preferably at room temperature and in a moisture- and oxygen-free environment [10]. Lee et al. have reported that a

decrease in the ALD deposition temperature prevents  $\text{Cu}_2\text{O}$  re-oxidation to  $\text{CuO}$  and facilitates the formation of a better quality heterojunction interface [9]. The lower  $V_{oc}$ s observed in Fig. 7(b) for  $\text{ZnO}$  deposited at 50 °C may be explained by the platen temperature not being sufficiently high for precursors to react on the substrate surface, leading to the  $\text{ZnO}$  film having poorer carrier properties. The best  $\text{ZnO}/\text{Cu}_2\text{O}$  solar cell was obtained with  $\text{ZnO}$  deposited at 100 °C for 100 s, and showed a 6-fold higher power conversion efficiency of 1.46% (see Figs. 1 and 6, Tables 1 and 2) for an optimized sample as compared to a standard  $\text{ZnO}/\text{Cu}_2\text{O}$  device. This performance is comparable with the  $\text{MgF}_2/\text{ITO}/\text{ZnO}/\text{Cu}_2\text{O}$  solar cell reported by Mittiga et al. [6], who deposited  $\text{ZnO}$  by ion beam sputtering on thermally oxidized  $\text{Cu}_2\text{O}$ . On the contrary, in this work, the heterojunction interface was formed outside a vacuum. The SEM image in Fig. 5b demonstrates that the optimized device surface was free of detrimental copper oxide compounds, in contrast to the device surface (Fig. 5a) formed using standard AALD  $\text{ZnO}$  deposition conditions which shows the presence of outgrowths (the  $\text{ZnO}$  conformally coats the  $\text{Cu}_2\text{O}$  and so the  $\text{ZnO}$  surface morphology reflects the  $\text{Cu}_2\text{O}$  morphology below).

### 3.3. External quantum efficiency measurements

To further investigate the effect of  $\text{CuO}$  formation on the quality of the heterojunction interface, external quantum efficiency

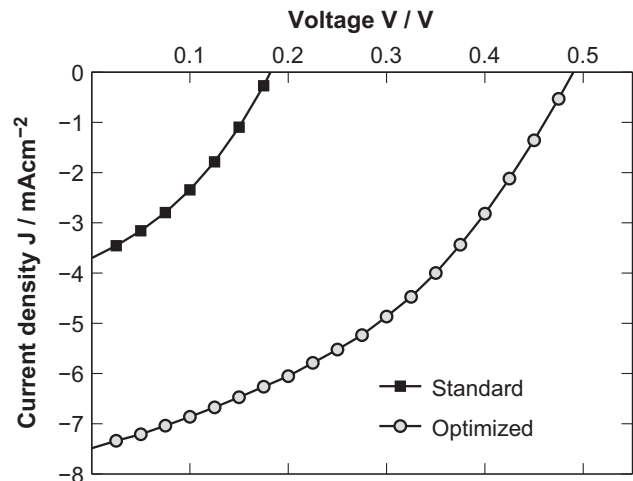


Fig. 6. Light current density–voltage ( $J$ – $V$ ) characteristics of the best  $\text{ITO}/\text{ZnO}/\text{Cu}_2\text{O}$  cells made using standard and optimized AALD conditions, measured at AM1.5G illumination (see Table 2).

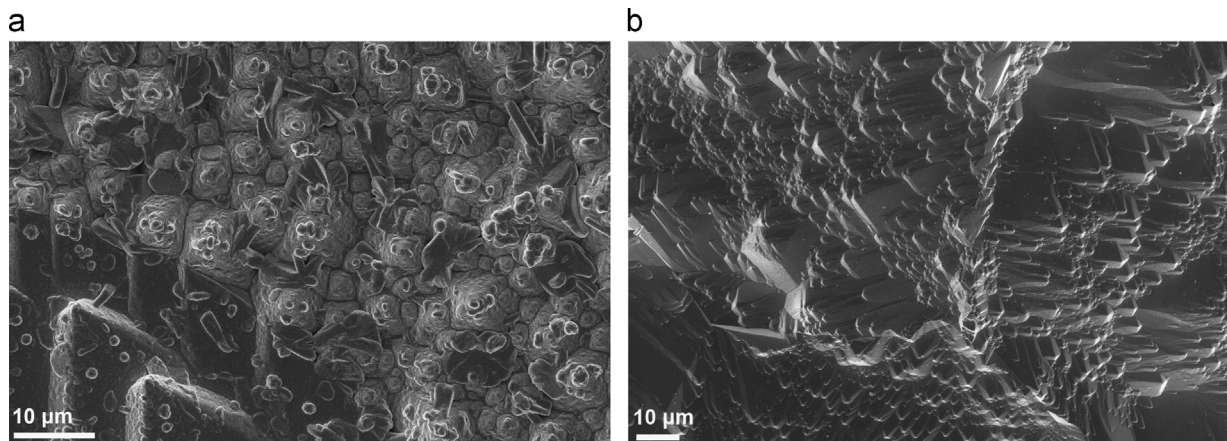


Fig. 5. SEM images of the top surface of  $\text{ZnO}/\text{Cu}_2\text{O}$  solar cells formed using (a) standard conditions and (b) optimized conditions of  $\text{ZnO}$  AALD deposition. Multiple whisker-, rod- and flower-like formations are present in the standard device.

measurements were performed on ZnO/Cu<sub>2</sub>O solar cells with ZnO deposited for 100 s at 100 °C and 150 °C. Since Cu<sup>2+</sup> defects present at the heterojunction interface due to CuO formation may act as mid-bandgap recombination centers, it is expected

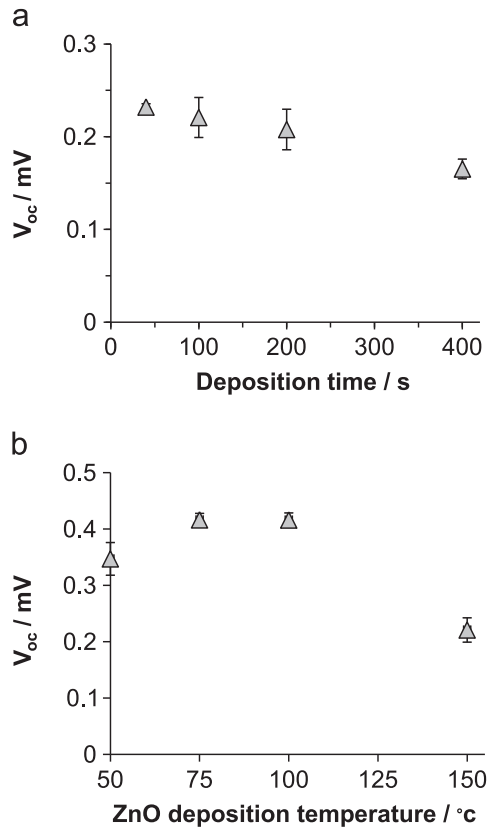


Fig. 7. Open-circuit voltage plotted versus (a) time and (b) temperature of ZnO deposition. Error bars represent standard error of the mean.

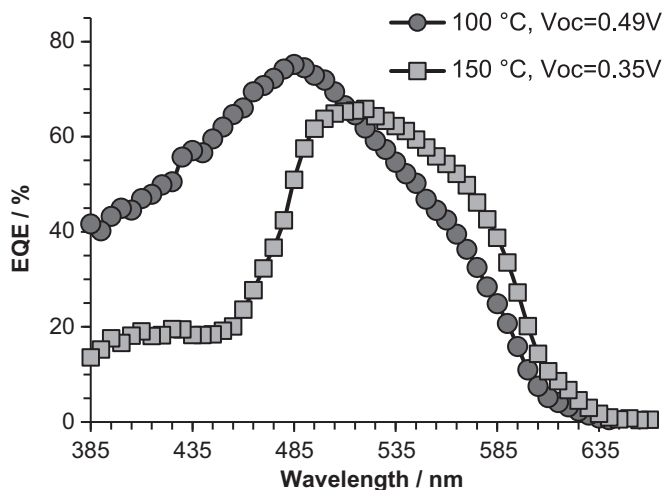


Fig. 8. EQE spectra of ZnO/Cu<sub>2</sub>O solar cells with ZnO deposited at 100 °C and 150 °C,  $V_{oc}$ s indicated.

that carriers generated close to the interface will be more likely to recombine in devices with more CuO formation. The absorption coefficient of Cu<sub>2</sub>O is such that radiation with a wavelength less than 475 nm is absorbed almost entirely within approximately 110 nm of the interface, whereas radiation of longer wavelengths (> 475 nm) is absorbed further from the junction [15]. From the EQE spectra of the ZnO/Cu<sub>2</sub>O solar cells in Fig. 8 one can see that the EQE at wavelengths below 475 nm correlated with the open-circuit voltage of the devices. Lower carrier collection efficiencies (for charges generated near the interface) were measured for the cell with lower  $V_{oc}$ . In contrast, the EQE at wavelengths above 475 nm was not dependent on the open-circuit voltage and instead was more affected by the bulk properties of Cu<sub>2</sub>O substrate. This is in agreement with our assertion that the low open-circuit voltage observed in these ZnO/Cu<sub>2</sub>O solar cells is a result of poor interface quality originating from the presence of CuO.

### 3.4. Mg incorporation into ZnO to further improve $V_{oc}$

It has been previously demonstrated that incorporating Mg into ZnO improves the open-circuit voltage of ZnO/Cu<sub>2</sub>O solar cells [16]. The Mg raises the conduction band of ZnO, increasing the maximum built-in potential attainable for the ZnO/Cu<sub>2</sub>O heterojunction [17]. Raising the conduction band of ZnO can also increase  $V_{oc}$ s by reducing the conduction band offset, which reduces interfacial recombination [18]. Therefore, Mg was incorporated into ZnO by introducing Mg precursor during the AALD deposition to further improve the  $V_{oc}$ . A solid solution with 21% Mg has been found to give the optimum balance between improved  $V_{oc}$  and reduced conductivity [7]. Similarly, as in the case of the undoped ZnO, the AALD deposition conditions were optimized for zinc magnesium oxide, and are detailed in Table 3. It was found that the optimized Zn<sub>0.79</sub>Mg<sub>0.21</sub>/Cu<sub>2</sub>O solar cells exhibited improved performance, with PCEs exceeding 2% and open-circuit voltages of 0.65 V for the champion devices. Table 3 and Fig. 9 present the performance of the best devices made with unannealed Cu<sub>2</sub>O

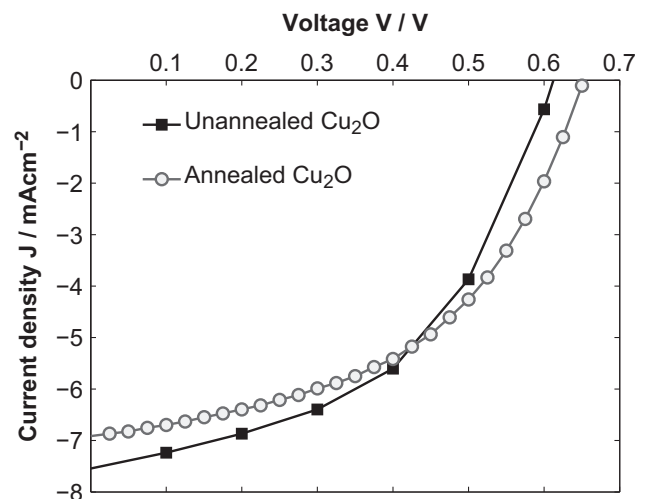


Fig. 9. Light  $J$ - $V$  characteristics for the best optimized ITO/Zn<sub>0.79</sub>Mg<sub>0.21</sub>O/Cu<sub>2</sub>O solar cells.

Table 3

Mg:ZnO AALD deposition parameters and performance of optimized ITO/Mg:ZnO/Cu<sub>2</sub>O solar cells.

Zn <sub>0.79</sub> Mg <sub>0.21</sub> /Cu <sub>2</sub> O solar cell	Deposition temperature (°C)	Deposition time (s)	$J_{sc}$ (mA/cm <sup>2</sup> )	$V_{oc}$ (V)	FF (%)	PCE (%)
Optimized (annealed Cu <sub>2</sub> O)	150	100	6.9	0.65	49.2	2.2
Optimized (unannealed Cu <sub>2</sub> O)	150	100	7.55	0.61	48.5	2.2

substrates, as well as substrates annealed at 1000 °C for 7 h at approximately 10,000 ppm oxygen partial pressure. This efficiency is the highest that has been reported for an ambient zinc oxide/cuprous oxide solar cell.

#### 4. Conclusion

ZnO/Cu<sub>2</sub>O heterojunctions have been successfully fabricated in air at low temperatures through the deposition of Zn<sub>1-x</sub>Mg<sub>x</sub>O by atmospheric ALD on thermally oxidized Cu<sub>2</sub>O. Oxidation of Cu<sub>2</sub>O to CuO prior to and during ZnO deposition was identified as the limiting factor to obtaining a high quality heterojunction interface. The presence of CuO led to a reduced open-circuit voltage due to the recombination at the Cu<sup>2+</sup> interface defects. Optimization of the Zn<sub>1-x</sub>Mg<sub>x</sub>O deposition conditions, including deposition temperature and time, in order to minimize substrate surface oxidation, led to a reduced amount of CuO at the Zn<sub>1-x</sub>Mg<sub>x</sub>O/Cu<sub>2</sub>O interface, and to the tripling of the open-circuit voltage, doubling of the short-circuit current density, and significantly improved PCEs of 2.2%. To the best of our knowledge, this is the first time that a ZnO/Cu<sub>2</sub>O heterojunction has been formed in atmosphere with device efficiency exceeding 2%. This highlights atmospheric (or spatial) ALD as a promising vacuum-free method for inexpensive and scalable fabrication of ZnO/Cu<sub>2</sub>O heterojunctions.

#### Acknowledgements

The authors would like to thank Dr. Nadia Stelmashenko for her assistance. The authors acknowledge the support of the Cambridge Overseas and Commonwealth Trust, the Rutherford Foundation of New Zealand, Girton College Cambridge and the ERC Advanced Investigator Grant, Novox, ERC-2009-adG247276 and EPSRC grant number RGS3717.

#### References

- [1] S. Rühle, A.Y. Anderson, H.N. Barad, B. Kupfer, Y. Bouhadana, E. Rosh-Hodesh, A. Zaban, All-oxide photovoltaics, *J. Phys. Chem. Lett.* 3 (2012) 3755–3764.
- [2] D.O. Scanlon, G.W. Watson, Undoped n-type Cu<sub>2</sub>O: fact or fiction? *J. Phys. Chem. Lett.* 1 (2010) 2582–2585.
- [3] T. Minami, Y. Nishi, T. Miyata, High-efficiency Cu<sub>2</sub>O-based heterojunction solar cells fabricated using a Ga<sub>2</sub>O<sub>3</sub> thin film as N-type layer, *Appl. Phys. Express* 6 (2013) 044101.
- [4] M. Ichimura, Y. Kato, Fabrication of TiO<sub>2</sub>/Cu<sub>2</sub>O heterojunction solar cells by electrophoretic deposition and electrodeposition, *Mater. Sci. Semicond. Process.* 16 (2013) 1538–1541.
- [5] D. Muñoz-Rojas, J. MacManus-Driscoll, Spatial atmospheric atomic layer deposition: a new laboratory and industrial tool for low-cost photovoltaics, *Mater. Horiz.* 1 (2014) 314.
- [6] A. Mittiga, E. Salza, F. Sarto, M. Tucci, R. Vasanthi, Heterojunction solar cell with 2% efficiency based on a Cu<sub>2</sub>O substrate, *Appl. Phys. Lett.* 88 (2006) 163502.
- [7] R.L.Z. Hoye, B. Ehrler, M.L. Böhm, D. Muñoz-Rojas, R.M. Altamimi A.Y. Alyamani, Y. Vaynzof, A. Sadhanala, G. Ercolano, N.C. Greenham R.H. Friend, J.L. MacManus-Driscoll, K.P. Musselman, Improved open-circuit voltage in ZnO–PbSe quantum dot solar cells by understanding and reducing losses arising from the ZnO conduction band tail (Early view), *Adv. Energy Mater.* (2014).
- [8] A.J. Kronemeijer, V. Pecunia, D. Venkateshvaran, M. Nikolka, A. Sadhanala, J. Moriarty, M. Szumilo, H. Siringhaus, Two-dimensional carrier distribution in top-gate polymer field-effect transistors: correlation between width of density of localized states and Urbach energy, *Adv. Mater.* 26 (2014) 728–733.
- [9] S.W. Lee, Y.S. Lee, J. Heo, S.C. Siah, D. Chua, R.E. Brandt, S.B. Kim, J.P. Mailoa, T. Buonassisi, R.G. Gordon, Improved Cu<sub>2</sub>O-based solar cells using atomic layer deposition to control the Cu oxidation state at the p–n Junction, *Adv. Energy Mater.* (2014).
- [10] T. Minami, T. Miyata, Y. Nishi, Efficiency improvement of Cu<sub>2</sub>O-based heterojunction solar cells fabricated using thermally oxidized copper sheets, *Thin Solid Films* 559 (2014) 105–111.
- [11] F. Biccari, *Defects and Doping in Cu<sub>2</sub>O*, Sapienza—University of Rome, 2009.
- [12] M. Nuys, J. Flohre, C. Leidinger, F. Köhler, R. Carius, Copper oxide nanoparticles for thin film photovoltaics, in: *MRS Proceedings*, 1494, 2013.
- [13] L. Papadimitriou, N.A. Economou, D. Trivich, Heterojunction solar cells on cuprous oxide, *Solar Cells* 3 (1981) 73–80.
- [14] T. Miyata, T. Minami, H. Tanaka, H. Sato, Effect of a Buffer Layer on the Photovoltaic Properties of AZO/Cu<sub>2</sub>O Solar Cells (603712–603711), *SPIE*, 2005.
- [15] K.P. Musselman, A. Wisnet, D.C. Iza, H.C. Hesse, C. Scheu, J.L. MacManus-Driscoll, L. Schmidt-Mende, Strong efficiency improvements in ultra-low-cost inorganic nanowire solar cells, *Adv. Mater.* 22 (2010) E254–E258.
- [16] T. Minami, Y. Nishi, T. Miyata, S. Abe, Photovoltaic properties in Al-doped ZnO/non-doped Zn<sub>1-x</sub>Mg<sub>x</sub>O/Cu<sub>2</sub>O heterojunction solar cells (MA2012-02), *ECS Trans.* (2012) 2886.
- [17] Z. Duan, A. Du Pasquier, Y. Lu, Y. Xu, E. Garfunkel, Effects of Mg composition on open circuit voltage of Cu<sub>2</sub>O–Mg<sub>x</sub>Zn<sub>1-x</sub>O heterojunction solar cells, *Sol. Energy Mater. Sol. Cells* 96 (2012) 292–297.
- [18] R.L.Z. Hoye, K.P. Musselman, J.L. MacManus-Driscoll, Research update: doping ZnO and TiO<sub>2</sub> for solar cells, *APL Mater.* 1 (2013) 060701.
- [19] K. Fujimoto, T. Oku, T. Akiyama, Fabrication and characterization of ZnO/Cu<sub>2</sub>O solar cells prepared by electrodeposition, *Appl. Phys. Express* 6 (2013) 086503.
- [20] Y.S. Lee, D. Chua, R.E. Brandt, S.C. Siah, J.V. Li, J.P. Mailoa, S.W. Lee, R.G. Gordon, T. Buonassisi, Atomic layer deposited gallium oxide buffer layer enables 1.2 V open-circuit voltage in cuprous oxide solar cells, *Adv. Mater.* (2014).
- [21] Y.S. Lee, J. Heo, S.C. Siah, J.P. Mailoa, R.E. Brandt, S.B. Kim, R.G. Gordon, T. Buonassisi, Ultrathin amorphous zinc-tin-oxide buffer layer for enhancing heterojunction interface quality in metal-oxide solar cells, *Energy Environ. Sci.* 6 (2013) 2112.
- [22] T. Minami, T. Miyata, K. Ihara, Y. Minamino, S. Tsukada, Effect of ZnO film deposition methods on the photovoltaic properties of ZnO–Cu<sub>2</sub>O heterojunction devices, *Thin Solid Films* 494 (2006) 47–52.
- [23] T. Minami, Y. Nishi, T. Miyata, J. Nomoto, High-efficiency oxide solar cells with ZnO/Cu<sub>2</sub>O heterojunction fabricated on thermally oxidized Cu<sub>2</sub>O Sheets, *Appl. Phys. Express* 4 (2011) 062301.
- [24] Y. Nishi, T. Miyata, T. Minami, The impact of heterojunction formation temperature on obtainable conversion efficiency in n-ZnO/p-Cu<sub>2</sub>O solar cells, *Thin Solid Films* 528 (2013) 72–76.
- [25] M. Izaki, T. Shinagawa, K.-T. Mizuno, Y. Ida, M. Inaba, A. Tasaka, Electrochemically constructed p-Cu<sub>2</sub>O/n-ZnO heterojunction diode for photovoltaic device, *J. Phys. D: Appl. Phys.* 40 (2007) 3326–3329.
- [26] T. Minami, H. Tanaka, T. Shimakawa, T. Miyata, H. Sato, High-efficiency oxide heterojunction solar cells using Cu<sub>2</sub>O sheets, *Japan. J. Appl. Phys.* 43 (2004) L917–L919.
- [27] A.T. Marin, D. Muñoz-Rojas, D.C. Iza, T. Gershon, K.P. Musselman, J. L. MacManus-Driscoll, Novel atmospheric growth technique to improve both light absorption and charge collection in ZnO/Cu<sub>2</sub>O thin film solar cells, *Adv. Functional Mater.* 23 (2013) 3413–3419.
- [28] S.S. Jeong, A. Mittiga, E. Salza, A. Masci, S. Passerini, Electrodeposited ZnO/Cu<sub>2</sub>O heterojunction solar cells, *Electrochimica Acta* 53 (2008) 2226–2231.